ESCUELA DE CONSTRUCCIÓN CIVIL
FACULTAD DE INGENIERÍA

Revista de la Construcción
Journal of Construction

*Research Article*

# Influences of nano-clay amount on flexure behavior of concrete identified by acoustic emission

**Sena Tayfur [1, *], Hasan Yavuz Ünal [2], Ninel Alver [1], Yeliz Pekbey [2]**

[1] Department of Civil Engineering, Ege University, Bornova (Türkiye), sena.tayfur@ege.edu.tr, ninel.alver@ege.edu.tr

[2] Department of Mechanical Engineering, Ege University, Bornova (Türkiye), hasan.yavuz.unal@ege.edu.tr, yeliz.pekbey@ege.edu.tr

*Correspondence: sena.tayfur@ege.edu.tr

**Received:** 17.09.2022; **Accepted:** 18.12.2023; **Published:** 25.04.2024

**Citation:** Tayfur, S., Yavuz, H., Alver, N., Pekbey, Y. (2024). Influences of nano-clay amount on flexure behavior of concrete identified by acoustic emission. Revista de la Construcción. Journal of Construction, 23(1), 5-15. https://doi.org/10.7764/RDLC.23.1.5

**Abstract:** Nano-modification is an effective method currently used to improve mechanical properties of concrete by adding various nanomaterials. The results obtained from previous studies demonstrate that presence of these particles has positive effects on both mechanical and durability performances of concrete. However, while the existing studies investigate the state of resistance, revealing progressive failure mechanism of nano-particle added concrete under loading is a significant subject. In this regard, Acoustic Emission (AE) method is useful for identification of invisible damage progress by means of basic phenomenon defined as release of energy due to a fracture and propagation of it as elastic waves in a stressed medium. Apart from the existing studies in the literature, this paper is focused on investigation of the influences of nano-clay on mechanical and failure behaviors of concrete by AE. For this purpose, a plain and three different concrete mixtures including 1%, 3% and 5% nano-clay (NC) of cement weight were prepared. 100x100x600 mm beam specimens were produced from these mixtures and were tested under three-point-bending. Furthermore, to reveal invisible failure mechanisms of the specimens, all tests were simultaneously monitored with AE method. The results reveal that presence of nano-clay increases the load capacity and ductility of the concrete specimens which is also confirmed by AE results, as more amount of micro-scale events are obtained.

**Keywords:** nano-clay, concrete, acoustic emission, fracture behavior, flexure.

## 1. Introduction

Enhancing the effects of nano-materials on the properties of polymer matrix composites has garnered researchers' attention for the usage of nano-materials in concrete as well. With the purpose of increasing strength and durability, and reducing pore size, nano-materials such as carbon nano-tube (CNT), titanium oxide, and nano-clay (NC) have been used as additives in the mixture of concrete (Norhasri et al, 2017). Several investigations exist in the literature focusing on the effects of the usage of nano-materials in concrete. Wang (2017) replaced nano-clay with 0.1%, 0.3%, and 0.5% of cement weight to evaluate compressive strength and thermal conductivity under ambient and high temperatures. Results indicate that both properties increased with increase in nano-clay content. However, when the test temperature exceeded 300°C, values of these properties did not improve. Du et al (2014) carried out a study on nano-silica-added concrete to observe the durability performance. Compressive strength of the nano-silica-added concrete was higher than that of plain concrete independently of the curing day. Another study was conducted by Assaedi et al (2016) in which geopolymer was combined with three different contents of nano-clay. Remarkable increments in flexural and compressive strengths were observed with a 2% nano-clay by weight. Compressive strength and porosity of concrete were found to be inversely proportional by Du et al (2015). They produced two types of lightweight concrete and applied compression tests after different curing times. According to the results, benefits of nano-silica decreased with increase in curing time. Afterwards, compressive and flexural strengths of concrete were investigated by Amin and El-Hassan (2015). They reinforced concrete with three different nano fillers: nano-silica, Ni-ferrite, and Cu-ferrite. The highest compressive and flexural strength were obtained from a 3% nano-silica replacement with cement by weight. In addition, epoxy-based polymer concrete was investigated by Niaki et al (2018).

Chopped basalt fiber and nano-clay were added, and the optimum content was selected according to compressive, flexural, splitting tensile, and impact tests. Nano-clay and basalt fiber almost increased all mechanical properties of the concrete. When the test temperature was above 250°C, there was no difference between nano-clay added and plain basalt fiber-reinforced polymer concretes. The effect of CNT was investigated by Morsy et al (2010). Firstly, cement was substituted with 6% meta nano-kaolin by weight, and five different CNT contents were blended with the mixture. Compressive strength of the cement increased with CNT fillers. The best result was obtained with a ratio of 0.02%. CNT was made cross-linked with the hydration product and resisted micro crack propagation. As a conclusion, compressive strength of the cement increased. Compressive strength of cement was increased with the addition of nano-clay. The reasons behind the compressive strength increment were pozzolanic activity and filler behavior of nano-clay (Heikal and Ibrahim, 2016). Additionally, concrete was reinforced with nano-silica due to its high surface activity, as indicated by Saloma et al (2015) and Khaloo et al (2016). Portland cement was replaced with nano-silica, and various mechanical tests were conducted by Saloma et al (2015). The presence of nano-silica increased compressive strength independently of curing time and corrosion resistance was also enhanced.

The effect of the smaller surface area of nano-silica was investigated by Khaloo et al (2016), revealing that smaller surface areas exhibited better compressive and splitting tensile strengths. Hybrid particles were incorporated into the concrete by replacing them with cement. 2% percent nano-silica by weight was combined with 5%, 8%, and 10% by weight of micro zeolite, and the mechanical and durability performances of the concrete were investigated. As the micro zeolite content increased, electrical resistance also increased; however, compressive strength and penetration of chloride ions decreased Eskandari et al (2015). In another study, Mahdikhani et al (2018) investigated the mechanical properties of nano-silica-added concrete in the acidic medium. It was observed that higher acidic levels led to a decrease in the compressive strength of the concrete. In addition, nano-silica has been shown to increase strength and reduce surface deterioration. According to Morsy et al (2011), the use of nano-clay reduces the need for cement and enhances the binding effect. This leads to the filling of micro voids, resulting in a denser material and increased compressive and flexural strengths of the cement paste. Anwar (2016) reported increase of 11% and 8% in compressive and flexural strengths for concrete with the presence of nano-clay. However, it was noted that the optimum value to avoid flocculation problems is to replace 3% of cement weight with nano-clay. Moreover, Chang et al.(2007) introduced nano-montmorillonite clay particles into the cement paste mixture at five different dosages and analyzed them at four different ages.

Their findings suggest that adding 0.6% and 0.4% nano-clay by the weight of cement yields optimal compressive strength and permeability coefficient. Results from Farzadnia et al (2013) indicates that the compressive strength of cement samples containing 2% and 3% halloysite nano-clay particles improved by up to 24% and 56%, respectively. Additionally, Mohammed et al (2018) evaluated the effects of nano-silica inclusion on the properties of pervious concrete, noting that workability is adversely affected. However, void ratio, permeability, and infiltration rate are decreased. Xu et al (2018) investigated the impacts of nano SiO2 and nano TiO2 particles on concrete samples. Their results indicate that even low-dosage nano particles can have distinctive positive effects on the durability of concrete. Hamed et al (2019) investigated the effects of nano-clay dispersion on split tensile, flexural, and bond strengths of concrete. According to their findings, the improvements in these properties ranged from 1.42 times to 3.74 times for different amounts of NC. In addition to the aforementioned studies, understanding the failure mechanisms of nano-particle-added concrete specimens with is a significant issue (Lorenzi et al, 2020). In this context, the Acoustic Emission (AE) technique proves to be valuable, being one of the nondestructive testing methods.

AE is a fundamental phenomenon defined as the release of energy from fractures and the propagation of these fractures as elastic waves in a stressed medium. This method has been applied in various fields for diverse purposes, including quality control for aircraft technology, detection of leakages in pressure vessels and pipes, characterization of damage types in different materials (Alver et al, 2017; Tayfur et al, 2018), and localization of invisible defects (Tayfur et al, 2023) such as cracks or delamination (Tayfur et al, 2018; Tayfur and Alver, 2019; Tayfur et al, 2023, Liu and Wei, 2024).

Application of AE technique on concrete is a developing subject. Moreover, its application on concrete strengthened with nano-materials is a more novel concern. Currently, only two studies on this subject exist in the literature: Barkoula et al (2016) incorporated nano-silica particles into cement mortars and investigated their failure processes using AE. Their results indicate that the inclusion of nano-silica particles increases amount of AE activities while the total energy remains unchanged. In another study, Nazerigivi et al (2017) examined the influence of nano-silica on the failure mechanisms of concrete specimens, revealing that nano-silica-added specimens exhibit more AE releases due to their higher heterogeneous structures.

As seen, these studies are limited to investigate the effects of nano-silica on concrete properties. However, when compared to other nano-materials, nano-clay emerges as the most cost-effective filler. Its affordability, coupled with its higher surface area, platelet morphology, and ability to interact with the matrix, has made nano-clay the focus of this study. This paper is focused on investigation on the effects of nano-clay on the mechanical and fracture properties of concrete by AE to identify invisible damage mechanisms. To achieve this goal, a plain and three different nano-clay-added concrete mixtures (containing 1%, 3%, and 5% nano-clay by cement weight) were prepared. Beam specimens measuring 100x100x600 mm were produced from these mixtures and tested under center-point bending after 28 days of curing. Additionally, to reveal the invisible failure mechanisms of the specimens and assess the effect of nano-clay content on these mechanisms, all tests were simultaneously monitored with the AE technique —an effective method for identifying active damages. Beyond the mechanical advantages, AE features of all specimens were also compared.

## 2. Materials and methods

### 2.1. *Acoustic emission (AE) methodology*

Acoustic emission (AE) is defined as transient stress waves propagating through a stressed material due to local fractures. To obtain data about active alterations in loaded members, recorded AE waves propagating within the member are converted into the digital signal forms, and parameters of these signals are analyzed. Firstly, to consider only meaningful signals apart from the noises, a “threshold” is set, as shown in Figure 1. "Amplitude" (the maximum voltage of the signal) is a frequently used AE parameter that provides insight into the magnitude of the damage. "Energy (measured area under the rectified signal envelope)" directly reflects the energy of the activity, which is the area of the signal envelope. "Duration" means the elapsed time between the first and last counts exceeding the threshold, while "rise time" defines the elapsed time between the first count and the count having the maximum amplitude. By evaluating time-based alterations of these parameters and/or their various combinations, significant information at critical points attributing to different mechanisms can be revealed such as matrix cracking, fiber rupturing, or steel yielding.

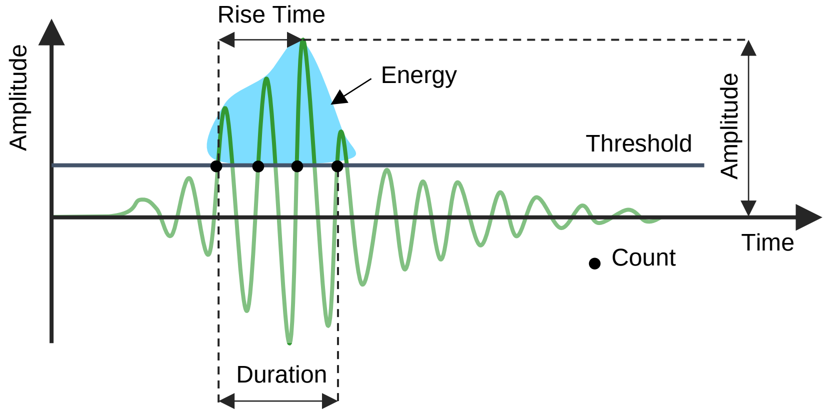


**Figure 1.** AE signal parameters.

By using these parameters, new AE features can be calculated and different analyses are conducted, parameter-based and signal-based analyses. By this means, time-based alterations of AE activities and their locations and types can be determined. RA value Eq. (1) is a seconder AE parameter identifying crack type. Higher RA values are attributed to shear-type activities (JCMS-IIIB5706, 2003).

$$RA\ value = \frac{Rise\ time}{Amplitude} \tag{1}$$

## 2.2. *Production of concrete mixtures*

Four different concrete mixtures were produced in the laboratory to investigate the effects of presence and amount of nano-clay on the mechanical and AE behaviors of concrete. Specifically, one mixture was nano-clay-free, while the others contained 1%, 3%, and 5% NC of the cement weight, as outlined in Table 1. The nano-clay-free mixture, labeled as NC0, was designed as conventional concrete with a cylinder compressive strength of 30 MPa and a water/cement ratio of 0.5. The other mixtures were formulated by adjusting the cement weight to incorporate the specified amounts of nano-clay. The binder used was CEM I 42.5 R type cement. The limestone aggregates (from Izmir) used included 0-3 mm, 5-15 mm, and 15-25 mm crushed limestone fractions, with gradation conforming to the limits specified in TS 8102 (2009) standards. The production process involved placing solid components into the mixer, followed by mixing. Water was then added, and the mixture was stirred for approximately 3 minutes. After incorporating the superplasticizer, the fresh concrete was ready for molding. Standard 100 x 100 x 600 mm prismatic specimens were formed from each mixture and compacted according to EN 12390-6 (2010) standard. The specimens were demolded the following day and subsequently cured for 28 days under standard conditions (20 ± 2 °C and 95% relative humidity).

**Table 1.** Contents of concrete mixture materials in kg/m$^3$.

| Component | | NC0 | NC1 | NC3 | NC5 |
|---|---|---|---|---|---|
| CEM I 42.5R | | 356 | 352 | 345 | 338 |
| Aggregate | 0-3mm | 940 | 940 | 940 | 940 |
| | 5-15mm | 385 | 385 | 385 | 385 |
| | 15-25mm | 573 | 573 | 573 | 573 |
| Water | | 178 | 178 | 178 | 178 |
| Superplasticizer | | 4.50 | 4.50 | 4.50 | 4.50 |
| Nano-clay | | - | 3.56 | 10.68 | 17.80 |

Organo modified montmorillonite (OMMT) nano-clay, characterized by its pure structure and ultra-white color, was employed as the nano material in concrete. Specifically, Esan Nano 1-140, extracted from the bentonite mine in the Kütahya-Eskişehir region of Turkey, was provided from Eczacıbaşı, Esan. Given that nano-clay is inherently hydrophilic, organic modification was undertaken to enhance its compatibility with organic materials and reduce water uptake. Following the organic modification process, the gaps between the layers increased, resulting in a more homogeneous mixture due to the platelet morphology and the presence of gaps (approximately ~40 Å). Particle dimensions were determined through particle size analysis, falling within the range of 0.5 to 15 µm, as detailed in Table 2. Chemical composition was also given in Table 2 (Cankaya and Sahin, 2019).

**Table 2.** Properties of ESAN NANO 1-140.

| Physical features | | | | |
|---|---|---|---|---|
| Property | Interlayer spacing (Å) | Partical sizes (µ) | | |
| Value | 36.62 | 50% of volume <2.7 | 82% of volume <5 | 100% of volume <15 |
| Chemical composition | | | | |
| TiO2 | LOI | SiO2 | Al2O3 | MgO |
| 45% | 45% | 44% | 6% | 1.4% |
| Na2O | Fe2O3 | CaO | K2O | |
| 0.6% | 0.4% | 0.4% | 0.3% | |

### 2.3. *Standard center-point-bending test*

To investigate the flexural behaviors of the specimens, center-point-bending tests were conducted on each specimen at the end of the 28th day, following the procedures outlined in TS 8102 (2009) standard. As illustrated in Figure 2, the span length of the configuration was 500 mm. A load, applied at the center of the mid-span with a loading speed of 0.2 mm/min, was administered using the Shimadzu AG-IS 100 kN Universal Testing Machine. Simultaneously, all tests were monitored using an eight-channel DiSP AE system by Mistras Group. Six AE sensors, resonating at 150 kHz, were strategically placed at different locations on the specimens using silicon grease. The detected signals were amplified using six preamplifiers with a gain of 40 dB and filtered based on a threshold of 40 dB. Throughout the tests, all AE activities were recorded and monitored.

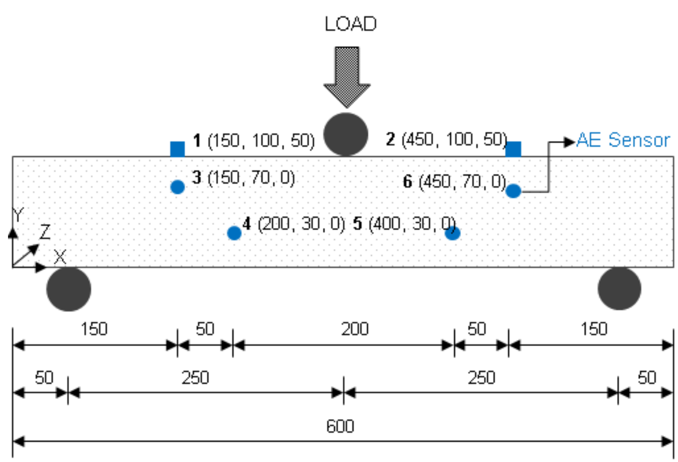


**Figure 2.** Center-point-bending test configuration and AE sensors (mm).

## 3. Results and discussion

### 3.1. *Mechanical behaviors*

Load vs. deflection curves of the test specimens under center-point-bending are presented in Figure 3.a. As observed, the plain concrete specimen NC0 carried a maximum load of 4431 N, while the presence of nano-clay elevated this capacity for the other three specimens. Accordingly, the ultimate load capacities for NC1, NC3, and NC5 were 4600 N, 5625 N, and 5875 N, respectively. Additionally, NC3 and NC5 exhibited 29% and 23% lower flexural displacements at their maximum load levels compared to the reference specimen (Table 3), and the toughness of all nano-clay-added specimens surpassed that of

NC0. The initial tangent modulus of elasticity also increased for specimens with 3% and 5% nano-clay by weight. Notably, while the modulus of elasticity of NC1 was the lowest, its toughness was the highest. The incorporation of decelerated crack propagation. Due to the platelet morphology of nano-clay, initiated cracks had to cover more distance to reach the surface of the specimen. The conditions of the specimens after their failures are illustrated in Figure 4.

The amount of nano-clay in the concrete mixture for this study was chosen based on existing literature findings for result comparison and behavior explanation using AE. As depicted in Figure 3.b, although NC5 resisted a 4% higher flexural load than NC3, its deflection at the maximum load is lower.

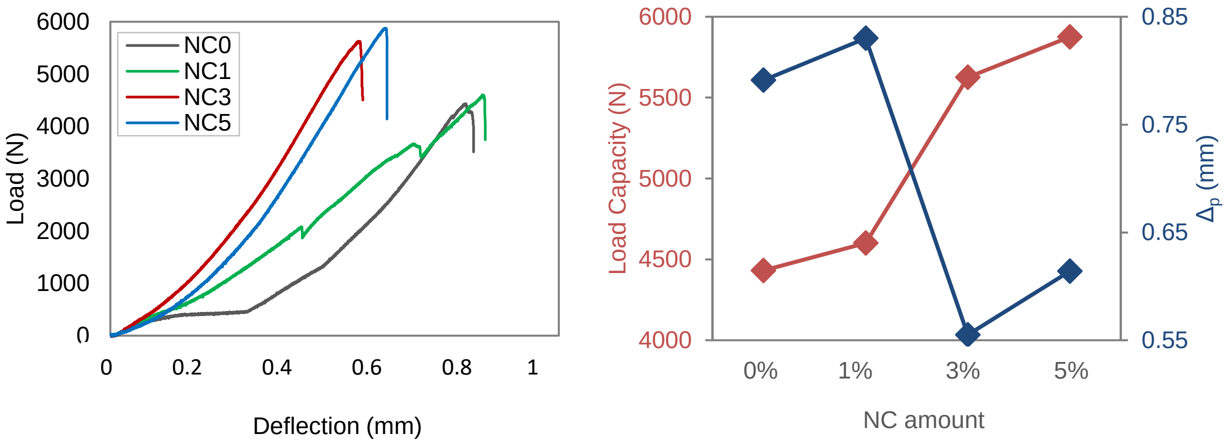


**Figure 3.** a) Load vs. deflection curves, and b) load vs. deflection relations at ultimate load levels.

**Table 3.** Mechanical results.

| Test specimen | Compressive strength (MPa) | Maximum load (N) | Deflection at max. load (mm) | Initial tangent modulus of elasticity (MPa) | Toughness (N×mm) |
|---|---|---|---|---|---|
| NC0 | 35.6 | 4431 | 0.79 | 3012.44 | 1211.48 |
| NC1 | 38.4 | 4600 | 0.83 | 2530.59 | 1737.70 |
| NC3 | 57.4 | 5625 | 0.56 | 3926.84 | 1337.47 |
| NC5 | 62.6 | 5875 | 0.61 | 4129.54 | 1427.78 |

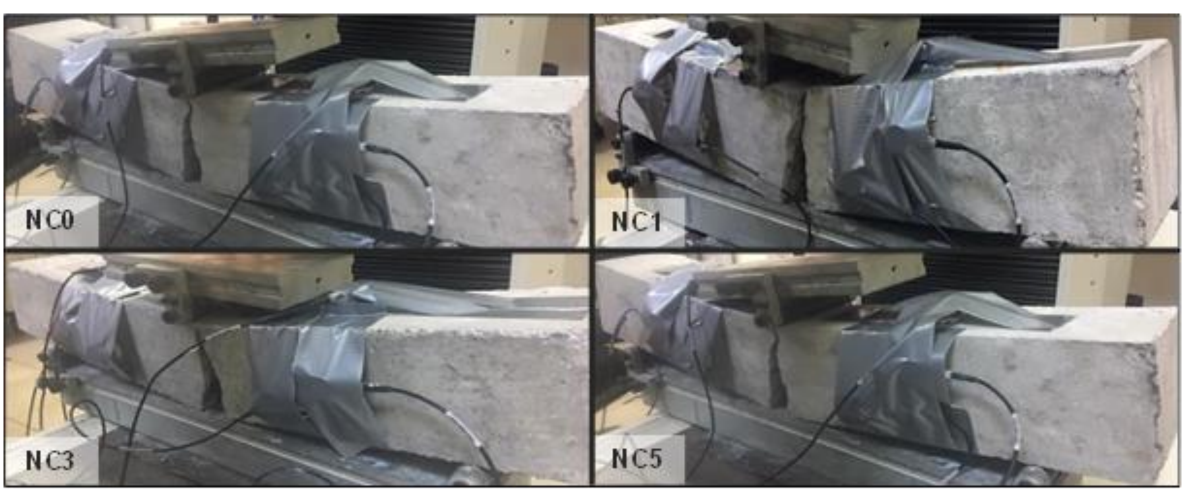


**Figure 4.** Failure of the test specimens after center-point-bending test.

*3.2. AE behaviors*

To compare the fracture of the test beams, their AE activities were investigated and evaluated. Prior to analysis, waveform-based amplitude-duration (A-D) and amplitude-rise time (A-RT) filtering, also known as Swansong II filters, were conducted to cleanse the noise-related AE data. Table 4 presents the limits used for filtering (Abdelrahman et al, 2015).

Totally 151, 282, 431 and 448 AE hits were recorded from NC0, NC1, NC3 and NC5, respectively. As seen, presence of nano-clay generated extra events, thus increased amount of the AE activities. Figure 5.a indicates AE hits in percentages with respect to deflection levels. Naturally, the largest parts of the activities of all beams originated when the load dropped. However, while 88% of AE hits were released suddenly in NC0 at that moment, this percentage decreased for the other three test beams. Besides, the least sudden AE hit release was in NC3 and NC5. Even though the total activities were higher in number for the nano-clay-added specimens compared with plain concrete specimen, they were distributed throughout the loading while the activities were concentrated at the load-drop-phase for the plain concrete specimen. This shows that addition of nano-clay distributed the fracture activities and led to a more ductile failure behavior.

**Table 4.** A-D & A-RT filtering limits (Abdelrahman et al, 2015).

| A-D Filter | | | | A-RT Filter | |
|---|---|---|---|---|---|
| Rejection limits | | Rejection limits | | Rejection limits | |
| Amp (dB) | Duration (µs) | Amp (dB) | Duration (µs) | Amp (dB) | Rise time (µs) |
| 40-44 | 400 | 66-70 | 1500 | 40-50 | 100 |
| 45-47 | 500 | 71-75 | 2500 | 51-60 | 200 |
| 48-52 | 600 | 76-80 | 3500 | 61-70 | 300 |
| 53-56 | 700 | 81-95 | 5000 | 71-100 | 400 |
| 57-60 | 800 | 96-100 | 10000 | - | - |
| 61-65 | 1000 | - | - | - | - |

Figure 5.b presents the cumulative AE energy distributions of the specimens. The presence of nano-clay resulted in higher AE releases, with the maximum total AE energy release observed in NC5. However, while NC0, NC1, and NC5 exhibited sudden AE energy releases at the load drop moment, the same pattern was not observed in NC3. Its cumulative AE energy curve was notably smoother before reaching the peak load.

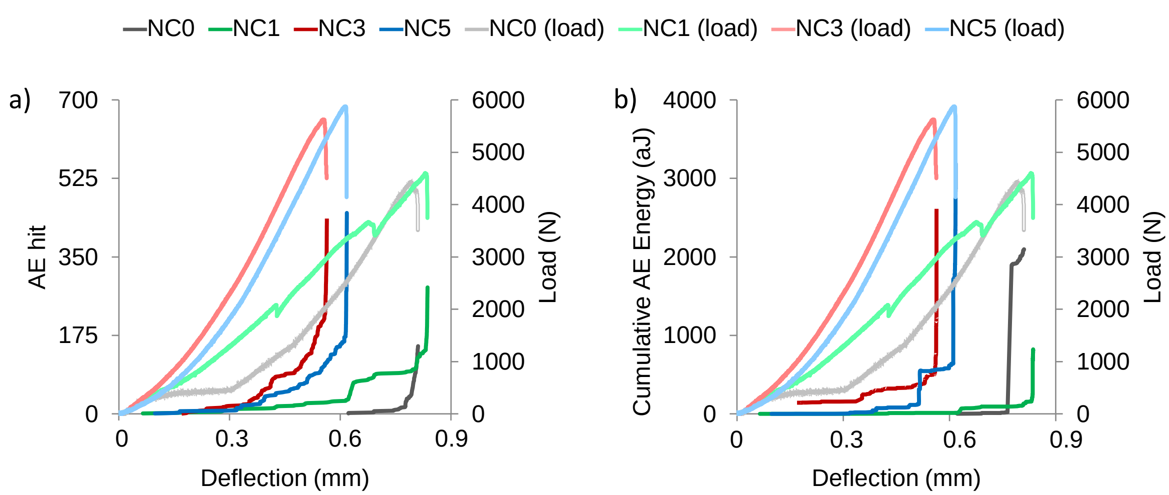


**Figure 5.** a) AE hits, b) cumulative AE energies.

To identify relevant crack locations corresponding to recorded AE hits, their arrival times at the sensors were utilized, and crack patterns of the specimens were drawn (Figure 6). The AIC picking algorithm and Geiger's method were employed to determine arrival time values and to locate AE hits. Notably, not only the locations but also the origination times of these activities were calculated and plotted based on deflection, considering the peak amplitude values of the events. As seen, with an increase in nano-clay content, the first AE event originated earlier. Furthermore, the originations of all AE activities extended over time, and their peak amplitude values decreased. This observation suggests that sudden alterations are mitigated, and more micro activities are generated.

Figure 7 illustrates the RA value distributions of the specimens based on their load vs. deflection behaviors. As seen, RA values of all specimens increased during the load-drop phase. However, these higher RA values were observed even at lower deflection levels in the nano-clay-added specimens. Specifically, higher RA values were observed at approximately the 0.65 mm deflection level for NC1, while they originated at approximately the 0.45 mm deflection level for NC3. In NC5, on the other hand, RA values of AE activities at these lower deflection phases were lower than those of NC1 and NC3. Consequently, the presence of nano-clay indicates that the signals recorded from nano-clay activities are perceived as shear-dominant type, leading to increased RA values. Additionally, the presence of nano-clay resulted in more micro-level damages up to the failure phase, as evidenced by the origination of high-RA value activities attributed to shear activities before the peak load. At this point, NC3 made the most substantial contribution.

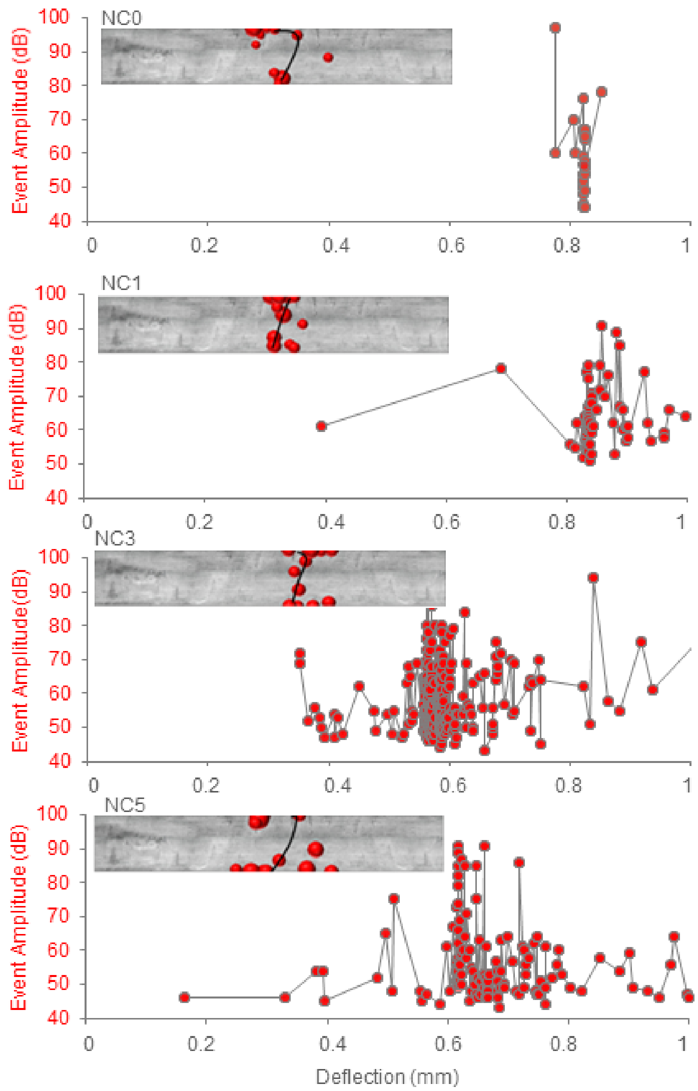


**Figure 6.** Peak amplitudes of the AE events and crack localization results.

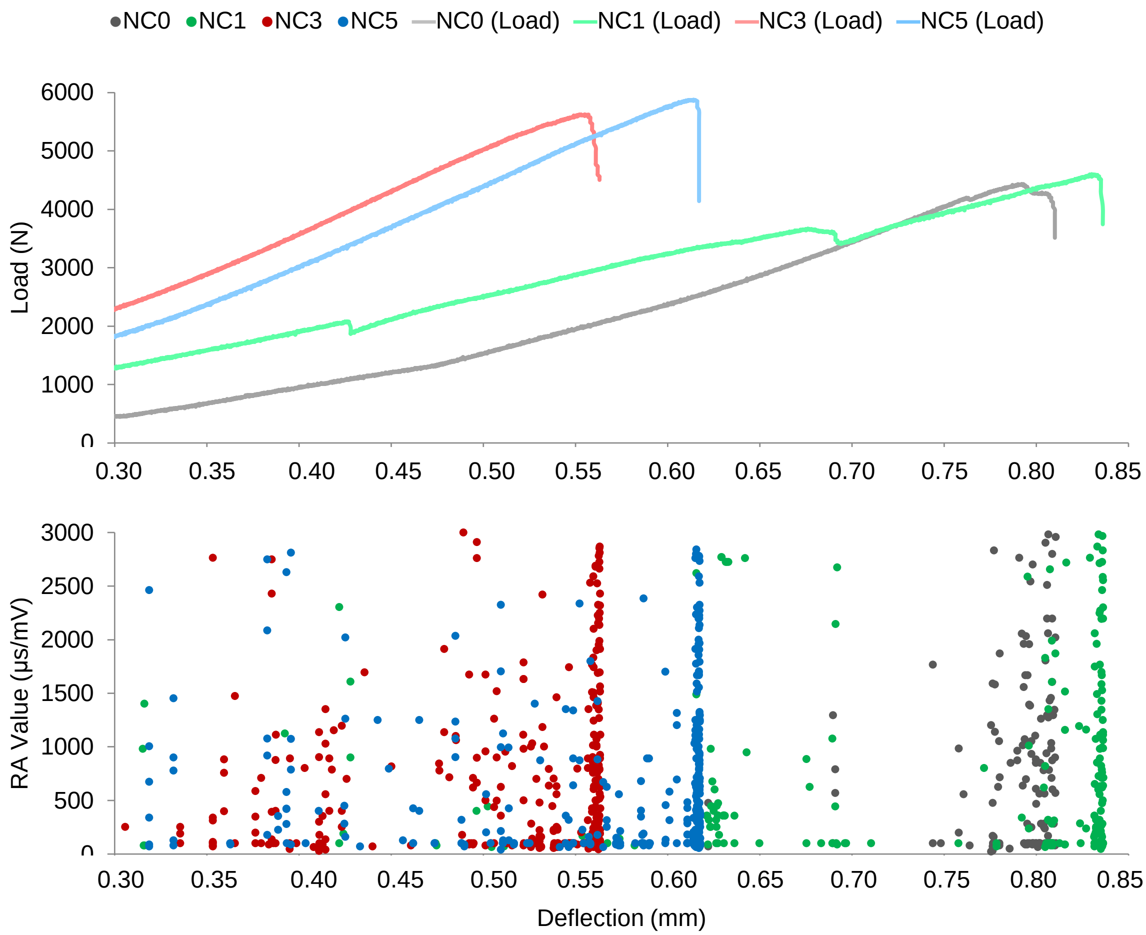


**Figure 7.** RA value variations of AE activities.

## 5. Conclusions

This paper aims to investigate the influence of nano-clay inclusion on the mechanical and failure behaviors of concrete using Acoustic Emission (AE). To achieve this objective, a plain concrete mixture and three distinct nano-clay added mixtures (comprising 1%, 3%, and 5% nano-clay by cement weight) were prepared. Beam specimens measuring 100x100x600 mm were cast from these mixtures and subjected to center-point-bending tests after 28 days of curing. Simultaneously, all tests were monitored using the AE technique, an effective method for identifying active damages and revealing otherwise invisible failure mechanisms. In addition to exploring the mechanical advantages, this study also compares the AE features of all specimens. The following conclusions were drawn from the investigation:

1. The presence of nano-clay increases the ultimate load capacity, maximum deflection and ductility of the concrete under flexure because crack propagations slow down. Thus, nano-clay is an effective addition to produce a high-strength and ductile concrete.
2. Invisible failure mechanisms of such type of structures produced from nano-clay added concrete can be monitored with AE. At this point, results of this study are useful indicators for evaluating AE behavior of nano-clay added concrete with its mechanical properties: Presence of nano-clay generates additional AE events, thus it increases amount of the AE activities. In addition, sudden damage alterations are prevented and an early warning feature for concrete is provided.
3. AE behaviors indicate that cumulative AE energy curve of the nano-clay added concrete specimens were rather smoother than that of plain concrete. Besides, with increase in nano-clay amount, first AE event originates earlier. In addition,

originations of all AE activities extend over time and their peak amplitude values decrease. This also shows sudden alterations are prevented and more and micro activities are provided.

4. Evaluating these AE findings, which were not observed from the mechanical results, is a useful approach to interpret the effect of nano-clay on scale and growth rate of the damage.

5. On the other hand, it is suggested that the RA value is also useful for scaling damage of the nano-clay added concrete with respect to AE activity type. The fact that the RA values in nano-clay added concrete are higher at earlier levels proves that more micro-damages occur before fracture.

**Author contributions:** Sena Tayfur: Conceptualization, Methodology, Investigation, Data curation, Writing, Editing. Hasan Yavuz Ünal: Conceptualization, Methodology, Investigation, Data curation, Writing. Ninel Alver: Conceptualization, Methodology, Investigation, Review, Editing, Supervision. Yeliz Pekbey: Conceptualization, Methodology, Review, Editing, Supervision, Material Supply.

**Acknowledgments:** Authors are grateful to Esan, Eczacıbaşı for material supply.

**Conflicts of interest:** The authors declare that there is no conflict of interest regarding the publication of this article.

## References

Abdelrahman, M., ElBatanouny, M. K., Ziehl, P., Fasl, J., Larosche, C., Frazcek, J. (2015). Classification of alkali–silica reaction damage using acoustic emission: A proof-of-concept study. Construction and Building Materials, 95, 406-413.

Alver, N., Tanarslan, H. M., Tayfur, S. (2017). Monitoring fracture processes of CFRP-strengthened RC beam by acoustic emission. Journal of Infrastructure Systems, 23(1), B4016002.

Amin, M., & El-hassan, K. A. (2015). Effect of using different types of nano materials on mechanical properties of high strength concrete. Construction and Building Materials, 80, 116–124.

Anwar, M. M. (2016). Influence of nano materials on flexural behavior and compressive strength of concrete. HBRC Journal, 12(2), 212-225.

Assaedi, H., Shaikh, F. U. A., & Low, I. M. (2016). Effect of nano-clay on mechanical and thermal properties of geopolymer. Journal of Asian Ceramics Society, 4, 19–28.

Barkoula, N. S., Ioannou, C., Aggelis, D. G., & Matikas, T. E. (2016). Optimization of nano-silica's addition in cement mortars and assessment of the failure process using acoustic emission. Construction and Building Materials, 125, 546-552.

Cankaya, N. & Sahin, R. (2019). Chitosan/clay bionanocomposites: structural, antibacterial, thermal and swelling properties. Cellulose Chem-istry and Technology, 53(5-6), 537-549.

Chang, T. P., Shih, J. Y., Yang, K. M., & Hsiao, T. C. (2007). Material properties of Portland cement paste with nano-montmorillonite. Journal of Materials Science, 42, 7478-7487.

Du, H., Du, S., & Liu, X. (2014). Durability performances of concrete with nano-silica. Construction and Building Materials, 73, 705–712.

Du, H., Du, S., & Liu, X. (2015). Effect of nano-silica on the mechanical and transport properties of lightweight concrete. Construction and Building Materials, 82, 114–122.

EN 12390-6. (2010). Concrete testing-hardened concrete - Part 4: Flexural strength test samples.

Eskandari, H., Vaghefi, M., & Kowsari, K. (2015). Investigation of Mechanical and Durability Properties of Concrete Influenced by Hybrid Nano Silica and Micro Zeolite. Procedia Materials Sciences, 11, 594–599. https://doi.org/10.1016/j.mspro.2015.11.084

Farzadnia, N., Ali, A. A. A., Demirboga, R., & Anwar, M. P. (2013). Effect of halloysite nanoclay on mechanical properties, thermal behavior and microstructure of cement mortars. Cement and Concrete Research, 48, 97-104. https://doi.org/10.1016/j.cemconres.2013.03.005

Hamed, N., El-Feky, M. S., Kohail, M., & Nasr, E. S. A. R. (2019). Effect of nano-clay de-agglomeration on mechanical properties of concrete. Construction and Building Materials, 205, 245-256.

Heikal, M., & Ibrahim, N. S. (2016). Hydration, microstructure and phase composition of composite cements containing nano-clay. Construction and Building Materials, 112, 19–27. https://doi.org/10.1016/j.conbuildmat.2016.02.177

JCMS-IIIB5706. (2003). Monitoring method for active cracks in concrete by acoustic emission. Federation of Construction Material Industries, Japan, 23-28.

Khaloo, A., Mobini, M. H., & Hosseini, P. (2016). Influence of different types of nano-SiO2 particles on properties of high-performance concrete. Construction and Building Materials, 113, 188–201. https://doi.org/10.1016/j.conbuildmat.2016.03.041

Liu, C., Wei, Y. (2024). Experimental investigation on damage of concrete beam embedded with sensor using acoustic emission and digital image correlation. Construction and Building Materials, 423, 135887. https://doi.org/10.1016/j.conbuildmat.2024.135887

Lorenzi, A., Stein, K., Reginatto, L. A., & da Silva, L. C. P. (2020). Concrete structures monitoring using ultrasonic tests. Revista de la Construccion, 19(3), 246-257. 10.7764/RDLC.19.3

Mahdikhani, M., Bamshad, O., & Shirvani, M. F. (2018). Mechanical properties and durability of concrete specimens containing nano silica in sulfuric acid rain condition. Construction and Building Materials, 167, 929–935. https://doi.org/10.1016/j.conbuildmat.2018.01.137

Mohammed, B. S., Liew, M. S., Alaloul, W. S., Khed, V. C., Hoong, C. Y., & Adamu, M. (2018). Properties of nano-silica modified pervious concrete. Case Studies in Construction, 8, 409-22.

Morsy, M. S., Alsayed, S. H., & Aqel, M. (2011). Hybrid effect of carbon nanotube and nano-clay on physico-mechanical properties of cement mortar. Construction and Building Materials, 25, 145–149. Morsy, S. A., Alsayed, S. H., & Aqel, M. (2010). Effect of nano-clay on mechanical properties and microstructures of ordinary Portland cement mortar. International Journal of Computer and Electrical Engineering, 10(01), 23-27.

Nazerigivi, A., Nejati, H. R., Ghazvinian, A., & Najigivi, A. (2017). Influence of nano-silica on the failure mechanism of concrete specimens. Computers and Concrete, 19(4), 429-434.

Niaki, M. H., Fereidoon, A., & Ahangari, A. M. G. (2018). Experimental study on the mechanical and thermal properties of basalt fiber and nanoclay reinforced polymer concrete. Composite Structures, 191, 231–238.

Norhasri, M. S. M., Hamidah, M. S., & Fadzil, A. M. (2017). Applications of using nano material in concrete: A review. Construction and Building Materials, 133, 91–97. Saloma, N. A., Imran, I., & Abdullah, M. (2015). Improvement of concrete durability by nanomaterials. Procedia Engineering, 125, 608–612. TS 8102. (2009). Design of concrete mixtures.

Tayfur, S., Alver, N. (2019). A 3D parameter correction technique for damage assessment of structural reinforced concrete beams by acoustic emission. Construction and Building Materials, 215, 148-161.

Tayfur, S., Alver, N., Abdi, S., Saatcı, S., Ghiami, A. (2018). Characterization of concrete matrix/steel fiber de-bonding in an SFRC beam: Principal component analysis and k-mean algorithm for clustering AE data. Engineering Fracture Mechanics, 194, 73-85.

Tayfur, S., Zhang, T., Mahdi, M., Issa, M., Ozevin, D. (2023). Cluster-based sensor selection framework for acoustic emission source localization in concrete. Measurement, 219, 113293.

Tayfur, S., Alver, N., Tanarslan, H. M., Ercan, E. (2018). Identifying CFRP strip width influence on fracture of RC beams by acoustic emission. Construction and Building Materials, 164, 864-876.

Tayfur, S.,Alver, N., Türk, E. Menteşoğlu, M., Ercan, E. (2023). Failure behavior of CFRP-strengthened reinforced concrete beam–column joints under reversed-cyclic lateral loading: mechanical and acoustic emission observations. Structural Engineering International, 1-12.

Wang, W. C. (2017). Compressive strength and thermal conductivity of concrete with nanoclay under various high-temperatures. Construction and Building Materials, 147, 305–311.

Xu, S., Xie, N., Cheng, X., Huang, S., Feng, L., Hou, P., & Zhu, Y. (2018). Environmental resistance of cement concrete modified with low dosage nano particles. Construction and Building Materials, 164, 535-553.